Original Article | Musculoskeletal Imaging

eISSN 2005-8330
https://doi.org/10.3348/kjr.2019.0241
Korean J Radiol 2019;20(10):1409-1421

Korean Journal of Radiology
KJR

Ultrasound Feature-Based Diagnostic Model Focusing on the "Submarine Sign" for Epidermal Cysts among Superficial Soft Tissue Lesions

Da Hyun Lee, MD[1], Choon-Sik Yoon, MD[1], Beom Jin Lim, MD[2], Hye Sun Lee, PhD[3], Sinae Kim, MS[3], A Lam Choi, MD[1], Sungjun Kim, MD[1]

[1]Department of Radiology, Gangnam Severance Hospital, Research Institute of Radiological Science, Center for Clinical Imaging Data Science, Yonsei University College of Medicine, Seoul, Korea; [2]Department of Pathology, Gangnam Severance Hospital, Yonsei University College of Medicine, Seoul, Korea; [3]Biostatistics Collaboration Unit, Yonsei University College of Medicine, Seoul, Korea

Objective: To develop a diagnostic model for superficial soft tissue lesions to differentiate epidermal cyst (EC) from other lesions based on ultrasound (US) features.

Materials and Methods: This retrospective study included 205 patients who had undergone US examinations for superficial soft tissue lesions and subsequent surgical excision. The study population was divided into the derivation set (n = 112) and validation set (n = 93) according to the imaging date. The following US features were analyzed to determine those that could discriminate EC from other lesions: more-than-half-depth involvement of the dermal layer, "submarine sign" (focal projection of the hypoechoic portion to the epidermis), posterior acoustic enhancement, posterior wall enhancement, morphology, shape, echogenicity, vascularity, and perilesional fat change. Using multivariable logistic regression, a diagnostic model was constructed and visualized as a nomogram. The performance of the diagnostic model was assessed by calculating the area under the curve (AUC) of the receiver operating characteristic curve and calibration plot in both the derivation and validation sets.

Results: More-than-half-depth involvement of the dermal layer (odds ratio [OR] = 3.35; $p = 0.051$), "submarine sign" (OR = 12.2; $p < 0.001$), and morphology (OR = 5.44; $p = 0.002$) were features that outweighed the others when diagnosing EC. The diagnostic model based on these features showed good discrimination ability in both the derivation set (AUC = 0.888, 95% confidence interval [95% CI] = 0.825–0.950) and validation set (AUC = 0.902, 95% CI = 0.832–0.972).

Conclusion: More-than-half-depth of involvement of the dermal layer, "submarine sign," and morphology are relatively better US features than the others for diagnosing EC.

Keywords: *Epidermal cyst; Submarine sign; Ultrasound; Nomogram*

INTRODUCTION

Epidermal cyst (EC), also called epidermoid cyst, infundibular cyst, or sebaceous cyst, is one of the common and benign cutaneous tumor-like lesions (1-5). It tends to remain asymptomatic and slowly grows as a benign dermal nodule with extremely rare malignant transformation (6-8). However, EC may become painful with the ulceration of the epithelial lining. This often precludes clinicians from differentiating EC from other symptomatic, superficially located soft tissue lesions (9, 10). Moreover, complete surgical excision of EC is required due to the high risk of

Received April 3, 2019; accepted after revision July 23, 2019.
This study was supported by the National Research Foundation of Korea (NRF) grant funded by the MIST (Ministry of Science and ICT) of Korean government (2017R1A2B2011366).
Corresponding author: Sungjun Kim, MD, Department of Radiology, Gangnam Severance Hospital, 211 Eonju-ro, Gangnam-gu, Seoul 06273, Korea.
• Tel: (822) 2019-3510 • Fax: (822) 3462-5472 • E-mail: agn70@yuhs.ac

recurrence (11). These characteristics of EC necessitate an accurate differential diagnosis. However, differentiating EC from other subcutaneous cysts, solid tumors, or vascular lesions is sometimes challenging (12). Many superficial lesions can be misdiagnosed as EC on the initial ultrasound (US) examination, partly because the incidence of EC has been reported to be the second-highest after lipoma (10).

In most clinical situations, US has been widely used as the first imaging modality owing to its superiority over MRI in terms of cost-effectiveness (9, 13-17). Nevertheless, to the best of our knowledge, the reported US features of EC could still not provide a definitive differential diagnostic point in practice (9, 12). Therefore, this study aimed to develop a diagnostic regression model for differentiating EC from other superficial soft tissue lesions based on their distinguishing US features and visualizing it as a nomogram to aid differential diagnosis.

MATERIALS AND METHODS

This retrospective study was approved by the Institutional Review Board of a single institution. The requirement for informed consent from patients was waived.

Patients

Patients who had palpable, superficial soft tissue lesions and underwent US examination before surgical excision, between January 2008 and October 2017, at our institution, were identified. The demographic characteristics of the patients were reviewed from the electronic medical records. Patients who underwent subsequent surgical excision and reported pathology were included in this study. Ineligible patients were excluded based on US image analysis by a senior musculoskeletal radiologist (reader A, 35 years of experience in musculoskeletal radiology) by using the following criteria: 1) mass with characteristic US finding of lipoma (18) and pathologically confirmed as such (19), and 2) mass occurring deep to the investing fascia (10). The flow chart illustrating patient selection is given in Figure 1.

US Examination

All US examinations were performed by an experienced musculoskeletal radiologist (reader B, 20 years of experience), using 5- to 12-MHz linear-arrayed transducers

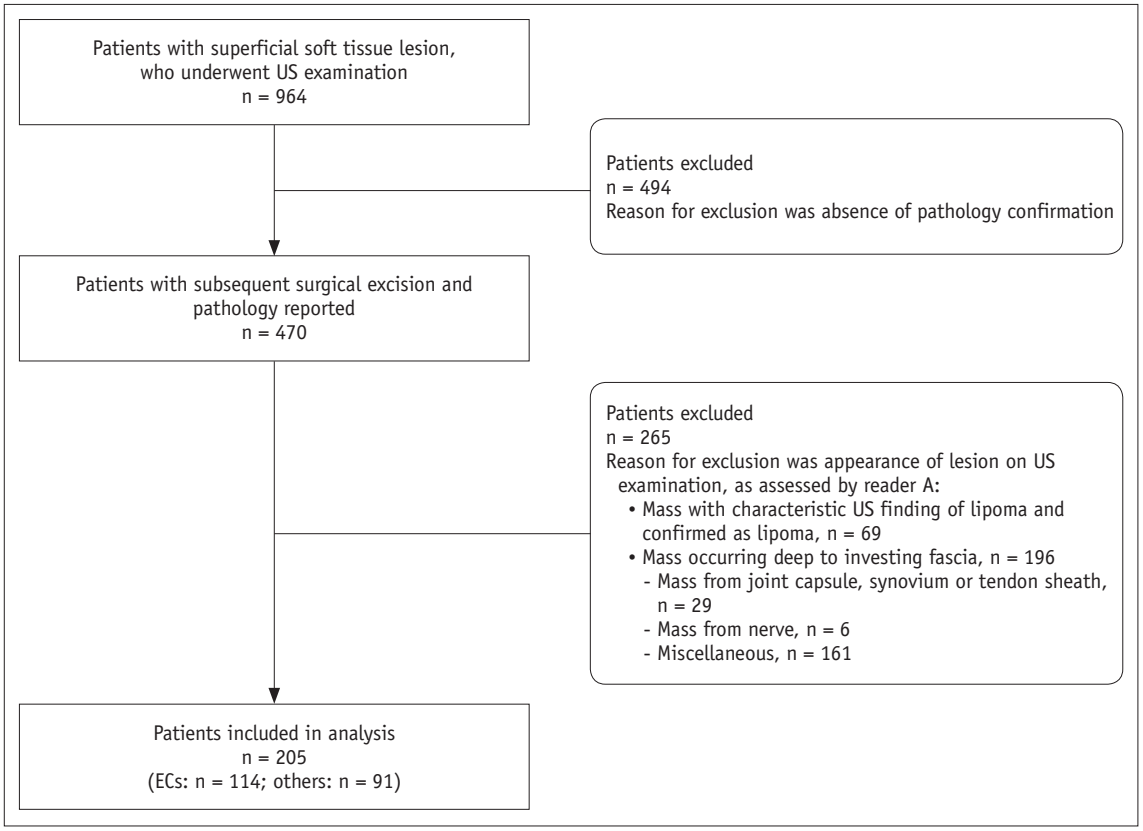

Fig. 1. Flow chart illustrating patient selection. EC = epidermal cyst, US = ultrasound

https://doi.org/10.3348/kjr.2019.0241

Korean Journal of Radiology
KJR

with the following systems: iU22 (Philips Medical Systems, New Hartford, CT, USA) or Aplio 500 (Canon Medical System, Tokyo, Japan).

The routine US protocol comprised gray-scale and color Doppler US examinations. The gray-scale image was obtained in the transverse and longitudinal planes for each lesion. Color Doppler study was performed after optimizing the visualization of minute vasculature and avoiding artifacts most of the time. The pulse-repetition frequency and wall filter were set as the lowest possible (20). Doppler gain was modulated to the maximum signal at the threshold to noise (21).

US Image Analysis

US Features as Variables

Two musculoskeletal radiologists (readers B and C, with 20 and 10 years of experience, respectively), blinded to the pathology results, independently evaluated each examination retrospectively. The US features of the lesions were described according to the following categories: whether the lesion involved more-than-half-depth of the dermal layer, whether the lesion showed the "submarine sign," presence of posterior acoustic enhancement, presence of posterior wall enhancement, morphology, shape, margin, echogenicity, vascularity, and presence of perilesional fat change. The evaluated categories are summarized in Table 1.

The location of the lesion was analyzed based on more-than-half-depth involvement of the dermal layer. The "submarine sign" is explained in detail in the following section. Posterior acoustic enhancement was defined as increased transmission deep through the lesion (22). Posterior wall enhancement was identified when the deepest wall of the mass appeared hyperechoic. The morphological category was evaluated based on the presence of a known morphological feature of EC (2, 23). The morphological classification of EC by Lee et al. (2) was used with modification for this purpose. Type 3 and 4 lesions, which were hypoechoic lesion with a central echogenic focus and inhomogeneously hypoechoic lesion, respectively, were excluded as the findings appeared nonspecific. In addition to the classification system stated above, "pseudotestis sign" of EC described by Huang et al. (23) was also used as a morphological indicator. The categories for shape and margin were adopted from the US lexicon concept from the fifth edition of the American Society of Radiology Breast Imaging Reporting and Data System (24) and modified for this study. The shape of the lesion was classified as oval, round, or irregular. Additionally, the margin of the lesion was classified as circumscribed, indistinct, or lobulated. Echogenicity was classified as hypoechogenicity, isoechogenicity, or hyperechogenicity as compared to the echogenicity of the adjacent hypodermal fat (17, 20). Vascularity of the lesion was evaluated on color Doppler images as absent, central, or peripheral. The presence of perilesional fat change was determined when the adjacent fat showed increased echogenicity to the deep hypodermal fat on the gray-scale image (25, 26) or increased signal as hyperemia on Doppler image (27).

Submarine Sign

We introduce a descriptive term "submarine sign," which

Table 1. US Characteristics of Superficial Soft Tissue Lesions

US Characteristics	Category Evaluation
More-than-half-depth involvement of dermal layer	Presence or absence
Submarine sign: Focal protrusion to epidermis	Presence or absence
Posterior acoustic enhancement	Presence or absence
Posterior wall enhancement	Presence or absence
Morphology: Alternating hypoechoic and hyperechoic concentric rings, predominantly hypoechoic lesion with central echogenic focus, lobulated lesion with area of varying echogenicity or pseudotestis pattern	Presence or absence
Shape	Oval, round or irregular
Margin	Circumscribed, indistinct or lobulated
Echogenicity	Hyperechogenicity, isoechogenicity or hypoechogenicity
Vascularity	No visible vascularity, central vascularity or peripheral vascularity
Perilesional fat change	Presence or absence

US = ultrasound

https://doi.org/10.3348/kjr.2019.0241

is depicted in detail in Figure 2 and provide suitable examples (Figs. 3, 4). The "submarine sign" is defined when the lesion shows focal projection of the hypoechoic portion, regardless of the width, depth, and morphology, towards the epidermis. EC may have a clinically visible punctum representing the follicular infundibulum of the terminal hair from which the cyst is derived (4, 5, 14, 28, 29). We speculated that the "submarine sign" may be related to the punctum (Fig. 2) and regarded it as a possible image feature of EC.

Statistical Analysis

The included patients were divided into the derivation and the validation sets according to the date of imaging (January 1, 2014) (30). Pearson's chi-square test or Fisher's exact test were performed to compare the categorical image variables between EC and other superficial lesions for categorical image variables. Interobserver agreement was assessed using Cohen's kappa statistics. Based on the derivation set data from reader B, multivariable logistic regression was performed to obtain the odds ratios (ORs) and *p* values to assess statistical significance (31, 32).

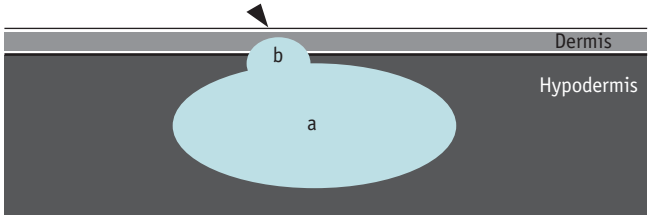

A

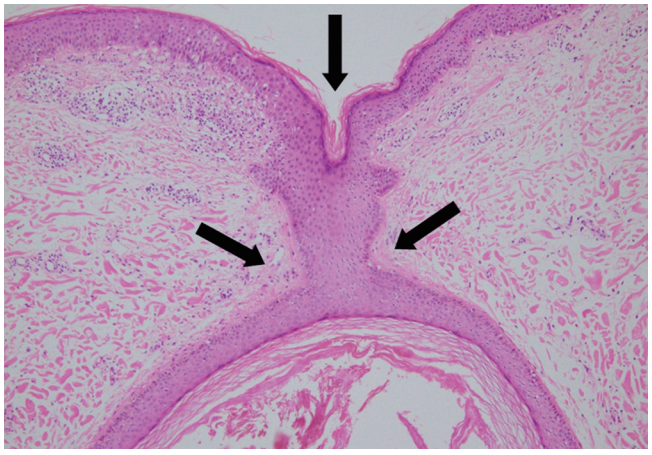

B

Fig. 2. "Submarine sign" of EC.
A. Illustration demonstrating "submarine sign," which is defined when lesion shows focal protrusion of hypoechoic portion (b) from main mass (a) to epidermis (arrowhead). **B.** Photomicrograph (original magnification, x 400; hematoxylin-eosin stain) shows focal tract-like appearance (arrows) of EC and epidermis.

A diagnostic model was developed and constructed as a nomogram. Through internal and external validations, we attempted to examine the performance of the diagnostic model (33, 34). The discriminatory ability of the diagnostic model was calculated using the area under the curve (AUC) of the receiver operating characteristic (ROC) curve. The Hosmer-Lemeshow test was used for testing the goodness of fit for the model. Moreover, a calibration plot was constructed to investigate the agreement between the observed outcomes and diagnostic prediction for the derivation and validation sets. For the derivation set, 200 bootstrap resampling was applied to obtain bias-corrected calibration (31). In contrast, the image variables constituting the diagnostic model were compared with the AUCs using the DeLong method to compare the predictive power of each variable. All statistical tests were two-tailed. A *p* value less than 0.05 indicated statistical significance with a 95% confidence interval (95% CI). In addition, a *p* value greater than or equal to 0.05 and less than 0.1 was considered as indicating a trend towards significance to

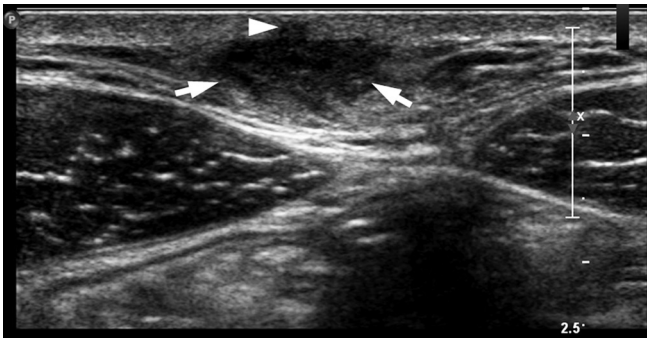

Fig. 3. Representative case of "submarine sign" in 54-year-old female with EC in back. Focal protrusion of hypoechoic portion (arrowhead) from main mass appears as "submarine sign." Arrows indicate delineation from adjacent hypodermal fat.

Fig. 4. Another representative case of "submarine sign" in 32-year-old male with EC in posterior neck. Focal protrusion of hypoechoic portion (arrowheads) from main mass appears like "tract-to-skin sign." It also counted as "submarine sign." Arrows indicate delineation from adjacent hypodermal fat.

https://doi.org/10.3348/kjr.2019.0241

Korean Journal of Radiology
KJR

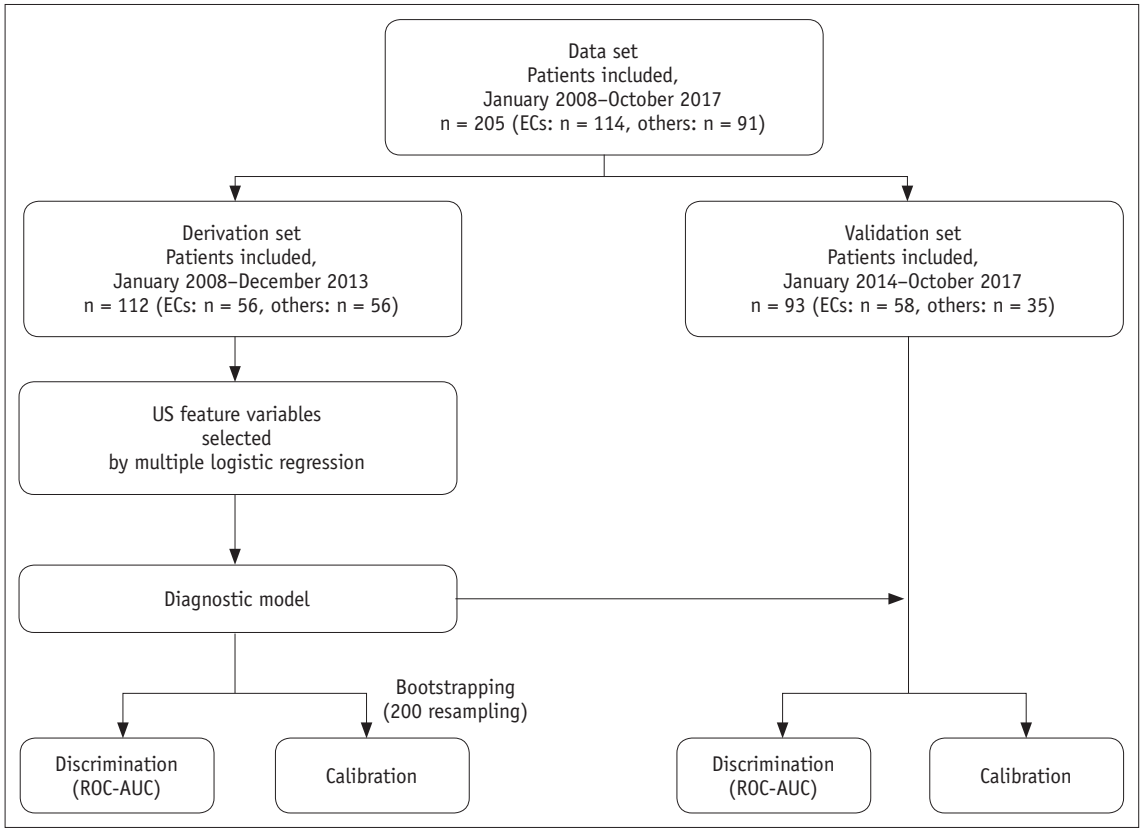

Fig. 5. Algorithm showing statistical analysis schema. AUC = area under curve, ROC = receiver operating characteristic

increase the sensitivity for detecting a potential selection bias. The statistical analysis scheme is given in Figure 5.

Statistical analysis was performed using SAS (version 9.3, SAS Institute Inc., Cary, NC, USA). The R Project for Statistical Computing (version 3.2.2, The R Foundation, Vienna, Austria, http://www.R-project.org) was used to develop the diagnostic model as a nomogram.

RESULTS

In the study period, 964 patients underwent US examinations for superficial soft tissue lesions, among whom, 470 patients underwent subsequent surgical excision and pathological examination. All patients had solitary lesions. As per our criteria, 265 patients were excluded for the following reasons: 1) mass with characteristic US finding of lipoma and pathologically confirmed as a lipoma (n = 69), and 2) mass present deep to investing fascia (n = 196). Finally, the study population comprised 205 dermal lesions from 205 patients.

For the derivation set, we identified 56 patients with pathologically confirmed EC (mean age, 37.3 years; 32 female patients and 24 male patients) between January 2008 and December 2013. Another 56 patients were pathologically confirmed as having other soft tissue disease (mean age, 43.9 years; 33 female patients and 22 male patients) during the same period. These 112 patients were included in the derivation set for the construction of the diagnostic model.

For the validation set, we identified 58 patients with pathologically confirmed EC (mean age, 37.0 years; 14 female patients and 44 male patients) between January 2014 and October 2017. Another 35 patients were pathologically confirmed as having other soft tissue disease (mean age, 36.7 years; 19 female patients and 16 male patients) during the same period. Finally, these 93 patients were included in the study as the validation set. The validation set was used to examine the performance of the diagnostic model.

Demographic characteristics of the study population are summarized in Table 2. Additionally, categorical evaluation of US exam in both sets from reader B is listed in Table 3.

Table 4 shows the interobserver agreement of US features among the two readers. High degree of agreement was shown for almost all variables, including more-than-half-depth involvement of the dermal layer (κ = 0.91), "submarine sign" (κ = 0.91), posterior wall enhancement

 https://doi.org/10.3348/kjr.2019.0241

Table 2. Demographic Data of Derivation and Validation Sets

Variable	Derivation Set				Validation Set			
	Total (n = 112)	EC (n = 56)	Others (n = 56)	*P*	Total (n = 93)	EC (n = 58)	Others (n = 35)	*P*
Age	40.6 ± 17.3	37.3 ± 16.3	43.9 ± 17.8	0.046	36.9 ± 16.0	37.0 ± 14.5	36.7 ± 18.5	0.949
Sex				0.848				0.003
Female	65 (58.0)	32 (57.1)	33 (58.9)		33 (35.5)	14 (24.1)	19 (57.1)	
Male	47 (41.2)	24 (42.9)	23 (41.0)		60 (64.5)	44 (75.9)	16 (42.9)	

Data for age are means ± standard deviation. Data for sex shows number of patients, with percentage in parentheses. EC = epidermal cyst

Table 3. Chi-Square Test or Fisher's Exact Test for Derivation and Validation Sets

Variable	Derivation Set			*P*	Validation Set			*P*
	Total (n = 112)	EC (n = 56)	Others (n = 56)		Total (n = 93)	EC (n = 58)	Others (n = 35)	
More-than-half-depth of dermal layer involvement				< 0.001				< 0.001
Presence	69 (61.6)	47 (83.9)	22 (39.3)		67 (72.0)	52 (89.7)	15 (42.9)	
Absence	43 (38.4)	9 (16.1)	34 (60.7)		26 (28.0)	6 (10.3)	20 (57.1)	
Submarine sign				< 0.001				< 0.001
Presence	45 (40.2)	40 (71.4)	5 (8.93)		40 (43.0)	36 (62.1)	4 (11.4)	
Absence	67 (59.8)	16 (28.6)	51 (91.1)		53 (57.0)	22 (37.9)	31 (88.6)	
Posterior acoustic enhancement				< 0.001				0.036
Presence	78 (69.6)	49 (87.5)	29 (51.8)		72 (77.4)	49 (84.5)	23 (65.7)	
Absence	34 (30.4)	7 (12.5)	27 (48.2)		21 (22.6)	9 (15.5)	12 (34.3)	
Posterior wall enhancement				0.115				0.004
Presence	72 (64.3)	40 (71.4)	32 (57.1)		62 (66.7)	45 (77.6)	17 (48.6)	
Absence	40 (35.7)	16 (28.6)	24 (42.9)		31 (33.3)	13 (22.4)	18 (51.4)	
Morphology				< 0.001				< 0.001
Presence	62 (55.4)	42 (75.0)	20 (35.7)		61 (65.6)	52 (89.7)	9 (25.7)	
Absence	50 (44.6)	14 (25.0)	36 (64.3)		32 (34.4)	6 (10.3)	26 (74.3)	
Shape				0.047				0.025
Oval	71 (63.4)	39 (69.6)	32 (57.1)		63 (67.7)	45 (77.6)	18 (51.4)	
Round	9 (8.0)	1 (1.8)	8 (14.3)		4 (4.3)	2 (3.5)	2 (5.7)	
Irregular	32 (28.6)	16 (28.6)	16 (28.6)		26 (28.0)	11 (19.0)	15 (42.9)	
Margin				0.443				0.061
Circumscribed	79 (70.5)	40 (71.4)	39 (69.6)		68 (73.1)	47 (81.0)	21 (60.0)	
Indistinct	14 (12.5)	5 (8.9)	9 (16.1)		16 (17.2)	8 (13.8)	8 (22.9)	
Lobulated	19 (17.0)	11 (19.6)	8 (14.3)		9 (9.7)	3 (5.2)	6 (17.1)	
Echogenicity				0.470				< 0.001
Hyper-	7 (6.3)	2 (3.6)	5 (8.9)		9 (9.7)	0 (0.0)	9 (25.7)	
Iso-	25 (22.3)	14 (25.0)	11 (19.6)		21 (22.6)	15 (25.9)	6 (17.1)	
Hypo-	80 (71.4)	40 (71.4)	40 (71.4)		63 (67.7)	43 (74.1)	20 (57.1)	
Vascularity				0.198				< 0.001
Negative	15 (13.4)	7 (12.5)	8 (14.3)		53 (57.0)	30 (51.7)	23 (65.7)	
Central	34 (30.4)	13 (23.2)	21 (37.5)		13 (14.0)	3 (5.2)	10 (28.6)	
Peripheral	63 (56.3)	36 (64.3)	27 (48.2)		27 (29.0)	25 (43.1)	2 (5.7)	
Perilesional fat change				0.004				0.119
Presence	51 (45.5)	33 (58.9)	18 (32.1)		36 (38.7)	26 (44.8)	10 (28.6)	
Absence	61 (54.5)	23 (41.1)	38 (67.9)		57 (61.3)	32 (55.2)	25 (71.4)	

Data are number of patients according to each US features, with percentage in parentheses.

https://doi.org/10.3348/kjr.2019.0241

Korean Journal of Radiology
KJR

(κ = 0.90), morphology (κ = 0.93), echogenicity (κ = 0.88), shape (κ = 0.93), margin (κ = 0.84), vascularity (κ = 0.92), and perilesional fat change (κ = 0.85). However, the kappa value for posterior acoustic enhancement indicated substantial agreement (κ = 0.77).

In the univariable regression, we considered variables that had *p* value less than 0.05, including more-than-half-depth involvement of the dermal layer (*p* < 0.001), "submarine sign" (*p* < 0.001), posterior acoustic enhancement (*p* < 0.001), morphology (*p* < 0.001), posterior wall enhancement (*p* = 0.117), and perilesional fat change (*p* = 0.005).

Thereafter, via stepwise multivariable logistic regression, more-than-half-depth involvement of the dermal layer (OR = 3.35; 95% CI = 0.99–11.3; *p* = 0.051), "submarine sign" (OR = 12.2; 95% CI = 3.46–42.8; *p* < 0.001), and morphology (OR = 5.44; 95% CI = 1.82–16.2; *p* = 0.002) were associated with EC. The result is listed in Table 5. Probability of EC can be calculated by using the following equation:

$$\text{Probability of EC} = \frac{1}{(1 + e^{-LP})}$$

where e is the exponential constant (e = 2.718), LP is the linear predictor, and

$$LP = -2.5768 + 1.2074 \times L + 2.4494 \times SM + 1.693 \times MP$$

where L is the value for whether the lesion involved more

Table 4. Inter-Reader Agreement on US Features from Kappa Statistics (95% CI)

Variable	κ (95% CI)
More-than-half-depth involvement of dermal layer	0.91 (0.82–0.99)
Submarine sign	0.91 (0.83–0.99)
Posterior acoustic enhancement	0.77 (0.64–0.90)
Posterior wall enhancement	0.90 (0.82–0.99)
Morphology	0.93 (0.86–0.99)
Shape	0.93 (0.86–0.99)
Margin	0.84 (0.74–0.94)
Echogenicity	0.88 (0.78–0.97)
Vascularity	0.92 (0.86–0.99)
Perilesional fat change	0.85 (0.76–0.95)

Data are κ values with 95% CIs in parentheses. 95% CI = 95% confidence interval

Table 5. Logistic Regression for US Features Predicting EC among Superficial Soft Tissue Lesions in Derivation Set

Variable	Univariable Analysis		Multivariable Analysis	
	OR (95% CI)	*P*	OR (95% CI)	*P*
More-than-half-depth involvement of dermal layer	8.07 (3.31–19.70)	< 0.001	3.35 (0.99–11.25)	0.051
Presence of submarine sign	25.5 (8.61–75.56)	< 0.001	12.2 (3.46–42.82)	< 0.001
Presence of morphology	5.40 (2.39–12.20)	< 0.001	5.44 (1.82–16.22)	0.002
Presence of posterior acoustic enhancement	6.52 (2.52–16.85)	< 0.001		
Presence of posterior wall enhancement	1.88 (0.86–4.11)	0.117		
Presence of perilesional fat change	3.03 (3.18–6.56)	0.005		

Data in parentheses are 95% CIs. OR = odds ratio

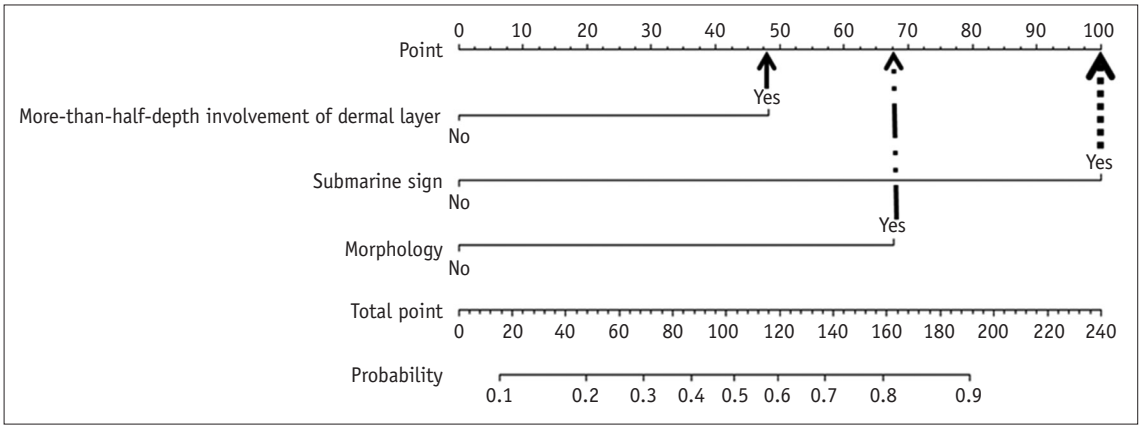

Fig. 6. Nomogram visualizing diagnostic model for predicting of EC. Point corresponding to each US feature can be determined using at uppermost scale (more-than-half-depth involvement of dermal layer = 48 [solid arrow]; "submarine sign" = 100 [dashed arrow]; and morphology = 68 [dotted and solid arrow]). Then, sum of all points is matched at scale of total point. Further, line drawn down from at that point helps calculate probability of EC. If calculated probability exceeds 0.44, it is considered highly likely to be EC.

https://doi.org/10.3348/kjr.2019.0241

than half the depth of the dermal layer (yes, L = 1; no, L = 0), SM is the value for the "submarine sign" (yes, SM = 1; no, SM = 0), and MP is the value for morphology (yes, MP = 1; no, MP = 0). A nomogram was constructed on the basis of the result of the stepwise multivariate analysis from the derivation set (Fig. 6). Via the summation of points of each variable, it was possible to estimate the probability by calculation of equation and visual assessment of the nomogram. The nomogram used for visual assessment is shown as examples in Figures 7 and 8.

The diagnostic model from the derivation set showed an excellent ability for discrimination (AUC = 0.888, 95% CI = 0.825–0.950; Hosmer-Lemeshow goodness-of-fit test, p = 0.656) (Fig. 9A) and calibration (Fig. 9B). The diagnostic model was applied to the external validation set and showed good ability for discrimination (AUC = 0.902, 95% CI = 0.832–0.972; Hosmer-Lemeshow goodness-of-fit test, p = 0.034) (Fig. 10A) and calibration (Fig. 10B).

By calculating the maximum Youden index and analyzing the ROC curve, we determined the optimal cut-off of the diagnostic model from the derivation set, which was 0.44. In the validation set, the diagnostic model showed 91.4% sensitivity (95% CI = 84.2–98.6), 77.1% specificity (95% CI = 63.2–91.1) and 86.0% accuracy (95% CI = 79.0–93.1). Likewise, in the derivation set, it showed 82.1% sensitivity (95% CI = 72.1–92.2), 85.7% specificity (95% CI = 76.5–94.9) and 83.9% accuracy (95% CI = 77.1–90.7). The detail of the estimation is given in Table 6.

By using DeLong method, we found that the "submarine sign" showed the highest predictive power (AUC = 0.813)

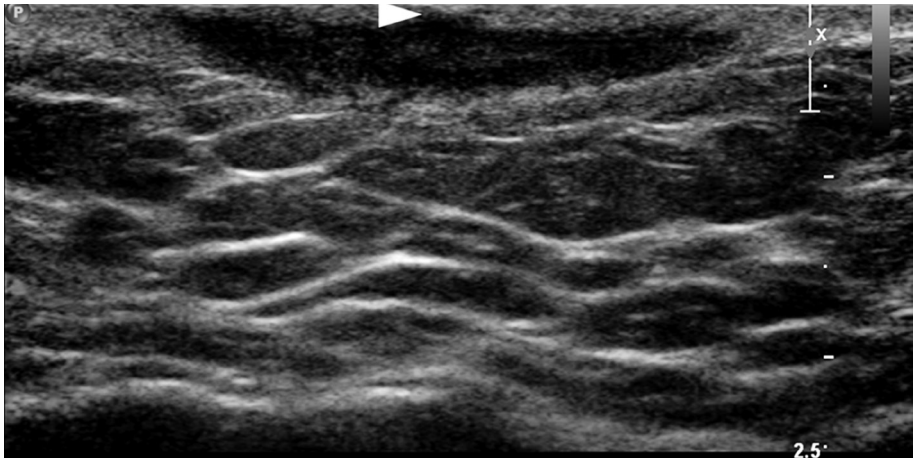

A

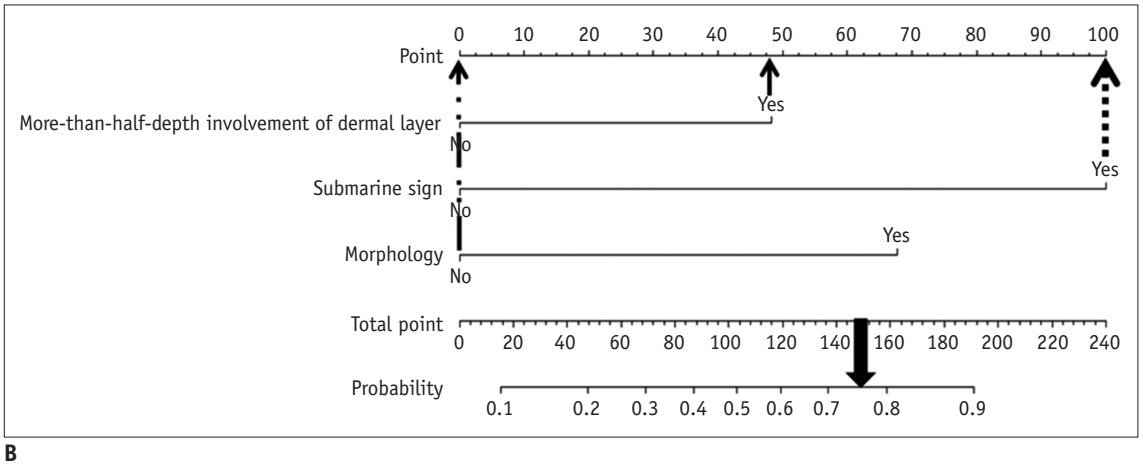

B

Fig. 7. True positive example identified using developed nomogram.
A. US exam obtained from 26-year-old male patient revealed subcutaneous nodule in anterior chest wall involving more-than-half-depth of dermal layer, "submarine sign" (arrowhead), and no posterior acoustic enhancement. Its morphology does not fit any of morphological criteria. **B.** Total point which is taken from nomogram of patient is 148 (48 + 100 + 0 = 148). This point is converted to predicted probability of 0.756 by using calculation of equation. Similar numerical value is obtained via visual assessment of nomogram (bold arrow). This lesion is pathologically confirmed as EC.

https://doi.org/10.3348/kjr.2019.0241

among the image variables, including more-than-half-depth involvement of the dermal layer (AUC = 0.723), posterior acoustic enhancement (AUC = 0.679), and morphology (AUC = 0.696) (Table 7).

DISCUSSION

Our study demonstrated that the distinguishing features of EC on US include more-than-half-depth involvement of the dermal layer (OR = 3.35), "submarine sign" (OR = 12.2) and morphology (OR = 5.44). The diagnostic model based on these US features suggests the presence of EC at the cutoff point of 0.44 with 91.4% sensitivity and 77.1% specificity for validation set and 82.1% sensitivity and 85.7% specificity for the derivation set. We believe that our diagnostic model could help differentiate EC from other superficial soft tissue disease on US.

Unlike previous investigations, we excluded the US finding of posterior acoustic enhancement from our diagnostic model. Posterior acoustic enhancement has

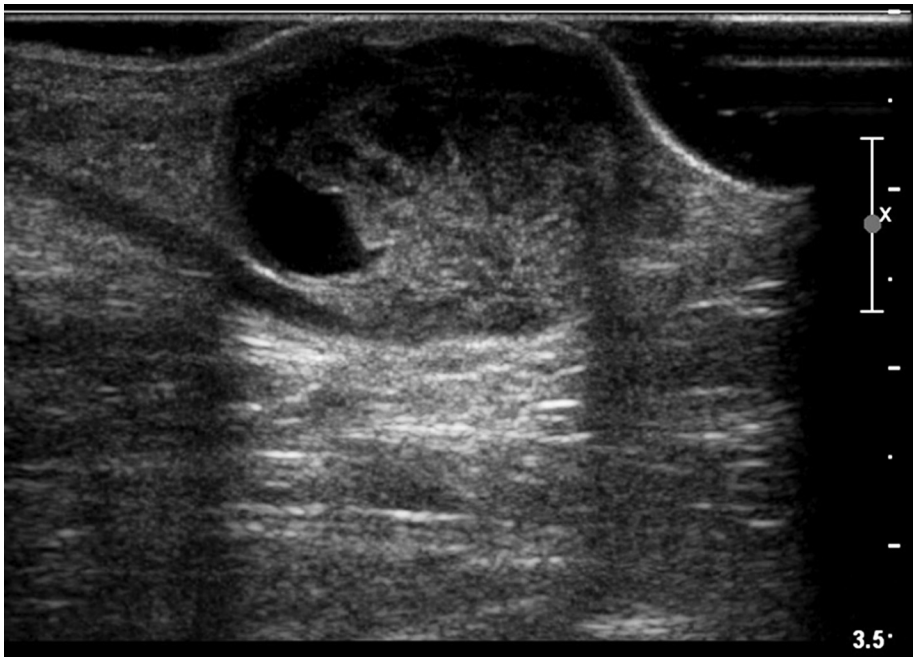

A

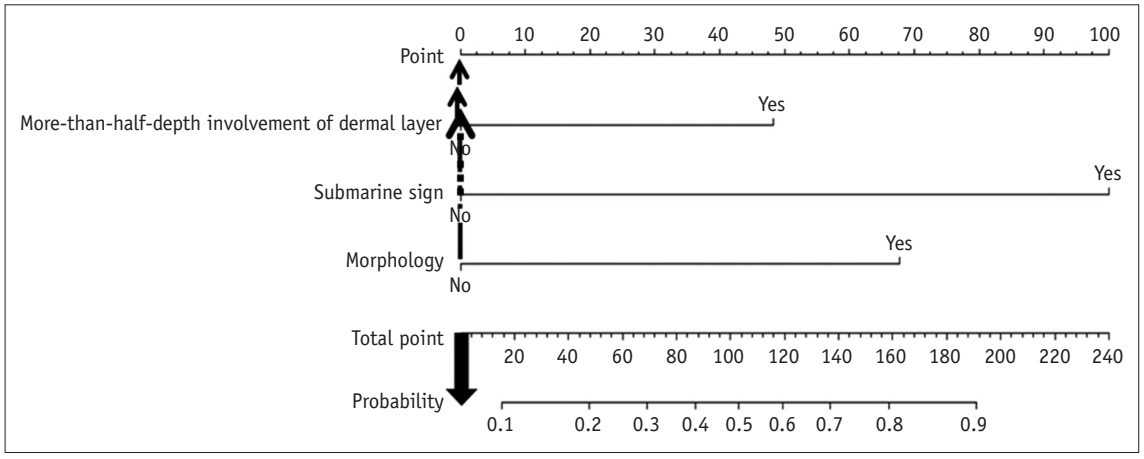

B

Fig. 8. True negative example identified using developed nomogram.
A. Subcutaneous nodule in left calf of 30-year-old male patient is noted with internal cystic change and posterior acoustic enhancement on US exam. However, this lesion shows less than half-depth involvement of dermis and no "submarine sign." Morphology of this lesion does not fit any of known typical morphology of EC. This mass was excised and was found to be schwannoma with cystic degeneration and hemorrhage. **B.** Total point obtained from nomogram of patient is 0 (0 + 0 + 0 = 0). As it yields predicted probability of 0.07 by using equation, visually assessed probability based on nomogram is less than 0.10 and lower than cut-off value of 0.44.

https://doi.org/10.3348/kjr.2019.0241

been reported as a diagnostically important feature in previous investigations (2, 3, 35). However, we excluded it because its predictive power was less than those of the other US features in the AUC analysis. Collinearity between 'morphology' and 'posterior acoustic enhancement' caused the discrepancy between our study and the previous investigations. Furthermore, morphology has been reported as an important feature for diagnosing EC. Huang et al. (23) emphasized the "pseudotestis appearance" of EC, which we used as a morphological indicator in this study. Moreover, the morphological features supported by pathologic findings in the study of Lee et al. (2), were also

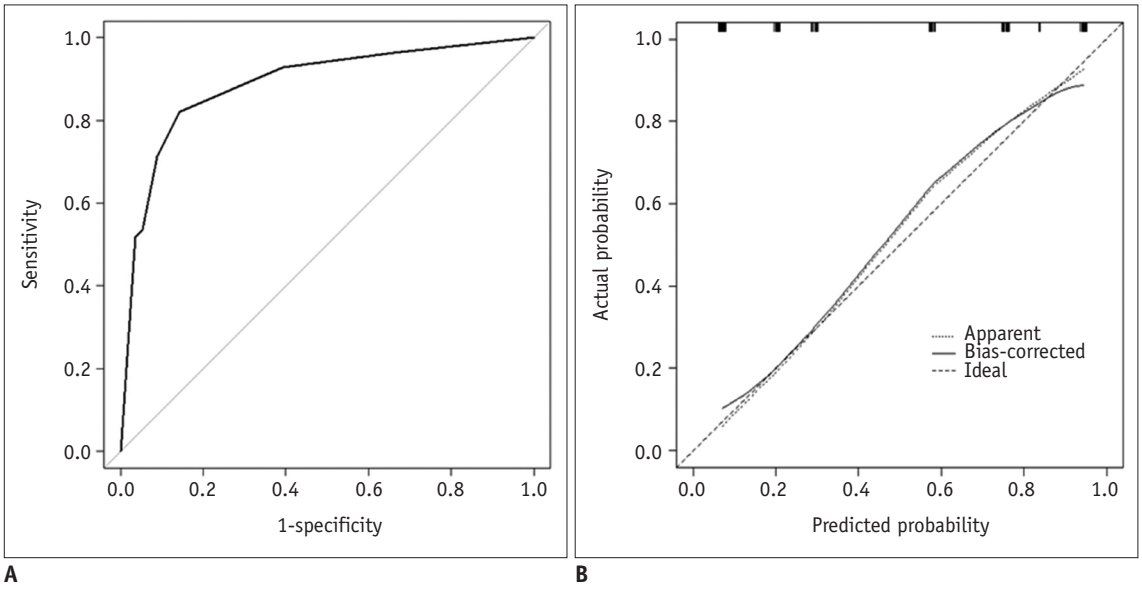

Fig. 9. Internal validation of diagnostic model.
A. Discrimination performance. Following ROC curve analysis for diagnostic model of EC was obtained in derivation set. AUC was 0.888 (95% CI, 0.825–0.950). **B.** Calibration ability. Dashed line was reference line where ideal diagnostic model would lie. Dotted line was calibration ability of diagnostic model, while solid line corrects for bias. 95% CI = 95% confidence interval

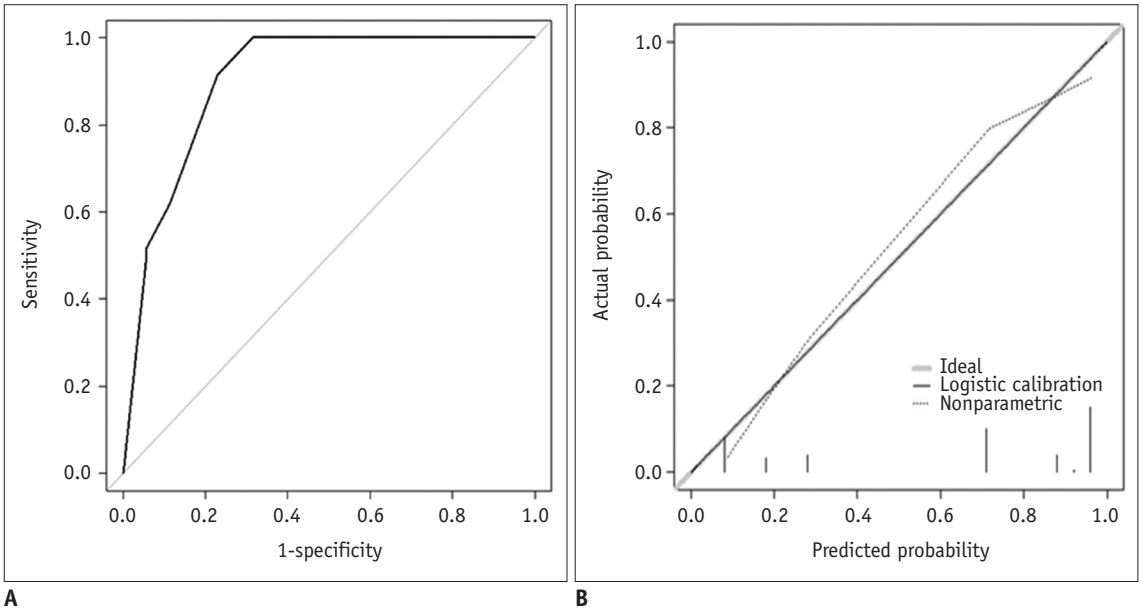

Fig. 10. External validation of diagnostic model.
A. Discrimination performance. In independent validation set, it was shown as following ROC curve analysis for diagnostic model of EC. AUC was 0.902 (95% CI, 0.832–0.972). **B.** Calibration ability. Soft and thickly drown diagonal line represents reference line where ideal diagnostic model would lie. Lines, that stand for calibration ability of diagnostic model in independent validation set with both logistic calibration (solid line) and nonparametric calibration (dotted line, using lowess), almost coincide with ideal reference.

https://doi.org/10.3348/kjr.2019.0241

Korean Journal of Radiology
KJR

Table 6. Estimation of Diagnostic Model by Using Cut-Off Value of 0.44

	True Positive	True Negative	False Positive	False Negative	AUC (95% CI)	Sensitivity (95% CI)	Specificity (95% CI)	Accuracy (95% CI)
Derivation set	46	48	8	10	0.888 (0.825–0.950)	82.1 (72.1–92.2)	85.7 (76.5–94.9)	83.9 (77.1–90.7)
Validation set	53	27	8	5	0.902 (0.832–0.972)	91.4 (84.2–98.6)	77.1 (63.2–91.1)	86.0 (79.0–93.1)

Data on true positive, true negative, false positive and false negative are number of patients. Data on sensitivity, specificity and accuracy are percentage with 95% CI in parentheses. AUC = area under curve

adopted in our study. Based on our results, we believe that morphology should be more focused than posterior acoustic enhancement in differentiating EC from other superficial soft tissue mass-like lesions.

Most of the ECs consisted of keratin debris and were lined with stratified squamous epithelium, arising from the follicular portion of the body (2, 3, 36). The presence of the tract towards the skin was previously inferred to represent the hair follicle of the dermis towards the epidermis of the EC (37). The "tract-to-skin sign" has been described and is presumably well known to radiologists and dermatologists as a representative characteristic of EC (14, 38), but this concept was not examined for its statistical significance. We believe that the "submarine sign" we have suggested in this study is closely related to the "tract-to-skin sign" with statistical consideration. The "submarine sign" is expected to be correlated with the punctum connecting the epidermis to the EC. Although the incidence of the punctum has not been rigorously investigated previously, to the best of our knowledge, the previous investigation did report the punctum in 40% of 34 EC (28). In this study, we did not directly correlate the punctum and the "submarine sign" in each case using radiopathologic comparison. However, we believe that the "submarine sign" could suffice as an important image feature based on the results of our study and previous studies describing the presence of the punctum histologically (28) and radiologically (23, 37).

Finally, the diagnostic model from our study shows 82.1% sensitivity and 85.7% specificity. At first glance, our diagnostic model seems to have a similar degree of sensitivity and specificity to those described in previous studies (9, 10). However, the study population itself differs from those of other studies because it only includes patients with lesions that require differential diagnosis owing to their similar appearance on US examination. Through the study design, we intentionally attempted to analyze the difference between EC and comparable lesions. As a result, lipomas and other deeply located soft tissue lesions were excluded. To our knowledge, the differentiating point between EC and similar lesions has not been reported previously. Furthermore, the reviewer who performed the exclusion did so only on the basis of the US finding without having access to any clinical information.

Table 7. Comparison of Predictive Power of Single Image Variable

Variable	AUC (95% CI)
More-than-half-depth involvement of dermal layer	0.723 (0.642–0.804)
Submarine sign	0.813 (0.742–0.883)
Posterior acoustic enhancement	0.679 (0.599–0.758)
Morphology	0.696 (0.611–0.782)

Data in parentheses are 95% CIs.

Several limitations of this study should be addressed. First, this study was retrospective. Hence, potential selection bias cannot be avoided. Characteristics such as more-than-half-depth involvement of the dermal layer and "submarine sign" could have been under detected as these features could be overlooked while acquiring the images used in this study. Second, the study population with EC was not further classified according to the existence of rupture. A ruptured EC is known to have giant cells with keratin material at the ruptured site on pathologic examination (2). Yuan et al. (39) reported that ruptured EC had lobulated margins rather than the oval- shaped margins seen in unruptured EC. However, Jin et al. (40) argued that the presence of a focal protrusion and not a lobulation in EC can serve as a feature for the differential diagnosis of ruptured and unruptured EC. However, the focal protrusion known as "submarine sign" can be applied to both ruptured and unruptured EC, because this sign is based on their possible developmental origin. In this study, we did not compare the exact location between a clinically visible punctum and the "submarine sign" in the lesions. Additionally, a ruptured EC may reveal more blood flow; hence, the value of a variable such as lesional vascularity may be low. Third, the accuracy of this diagnostic model

 https://doi.org/10.3348/kjr.2019.0241

with a cut off value of 0.44 could be limited because the actual prevalence of EC could not be reflected in this study population. Therefore, our current model needs to be further assessed for its diagnostic performance by using data from other populations.

In conclusion, more-than-half-depth involvement of the dermal layer, presence of "submarine sign," and morphology has a strong association with EC. The "submarine sign" is a useful US marker for EC, even though it has not been validated with pathologic diagnosis in each case. The nomogram developed in our study is expected to contribute as a quantitative tool for the differential diagnosis of EC, thereby aiding therapeutic decision-making.

Conflicts of Interest

The authors have no potential conflicts of interest to disclose.

ORCID iDs

Sungjun Kim
https://orcid.org/0000-0002-7876-7901
Da Hyun Lee
https://orcid.org/0000-0001-7593-0403
Choon-Sik Yoon
https://orcid.org/0000-0003-2010-6710
Beom Jin Lim
https://orcid.org/0000-0003-2856-0133
Hye Sun Lee
https://orcid.org/0000-0001-6328-6948
Sinae Kim
https://orcid.org/0000-0002-9900-492X
A Lam Choi
https://orcid.org/0000-0002-0325-4802

REFERENCES

1. Vincent LM, Parker LA, Mittelstaedt CA. Sonographic appearance of an epidermal inclusion cyst. *J Ultrasound Med* 1985;4:609-611
2. Lee HS, Joo KB, Song HT, Kim YS, Park DW, Park CK, et al. Relationship between sonographic and pathologic findings in epidermal inclusion cysts. *J Clin Ultrasound* 2001;29:374-383
3. Kim HK, Kim SM, Lee SH, Racadio JM, Shin MJ. Subcutaneous epidermal inclusion cysts: ultrasound (US) and MR imaging findings. *Skeletal Radiol* 2011;40:1415-1419
4. Stone MS. *Cysts*. In: Bolognia JL, Schaffer JV, Cerroni L, eds. *Dermatology*, 4th ed. New York, NY: Elsevier, 2018:1917-1929
5. *Benign neoplasms and hyperplasias*. In: Wolff K, Johnson RA, Saavedra AP, Roh EK, eds. *Fitzpatrick's color atlas and synopsis of clinical dermatology*, 8th ed. New York, NY: McGraw-Hill Education, 2017:141-173
6. López-Ríos F, Rodríguez-Peralto JL, Castaño E, Benito A. Squamous cell carcinoma arising in a cutaneous epidermal cyst: case report and literature review. *Am J Dermatopathol* 1999;21:174-177
7. Veenstra JJ, Choudhry S, Krajenta RJ, Eide MJ. Squamous cell carcinoma originating from cutaneous cysts: the Henry Ford experience and review of the literature. *J Dermatolog Treat* 2016;27:95-98
8. Antón-Badiola I, San Miguel-Fraile P, Peteiro-Cancelo A, Ortiz-Rey JA. [Squamous cell carcinoma arising on an epidermal inclusion cyst: a case presentation and review of the literature]. *Actas Dermosifiliogr* 2010;101:349-353
9. Hwang EJ, Yoon HS, Cho S, Park HS. The diagnostic value of ultrasonography with 5-15-MHz probes in benign subcutaneous lesions. *Int J Dermatol* 2015;54:e469-e475
10. Hung EH, Griffith JF, Ng AW, Lee RK, Lau DT, Leung JC. Ultrasound of musculoskeletal soft-tissue tumors superficial to the investing fascia. *AJR Am J Roentgenol* 2014;202:W532-W540
11. Nigam JS, Bharti JN, Nair V, Gargade CB, Deshpande AH, Dey B, et al. Epidermal cysts: a clinicopathological analysis with emphasis on unusual findings. *Int J Trichology* 2017;9:108-112
12. Apollos JR, Ekatah GE, Ng GS, McFadyen AK, Whitelaw SC. Routine histological examination of epidermoid cysts; to send or not to send? *Ann Med Surg (Lond)* 2016;13:24-28
13. Kuwano Y, Ishizaki K, Watanabe R, Nanko H. Efficacy of diagnostic ultrasonography of lipomas, epidermal cysts, and ganglions. *Arch Dermatol* 2009;145:761-764
14. Wortsman X. Common applications of dermatologic sonography. *J Ultrasound Med* 2012;31:97-111
15. Wortsman X, Wortsman J. Clinical usefulness of variable-frequency ultrasound in localized lesions of the skin. *J Am Acad Dermatol* 2010;62:247-256
16. Kleinerman R, Whang TB, Bard RL, Marmur ES. Ultrasound in dermatology: principles and applications. *J Am Acad Dermatol* 2012;67:478-487
17. Toprak H, Kiliç E, Serter A, Kocakoç E, Ozgocmen S. Ultrasound and Doppler US in evaluation of superficial soft-tissue lesions. *J Clin Imaging Sci* 2014;4:12
18. Fornage BD, Tassin GB. Sonographic appearances of superficial soft tissue lipomas. *J Clin Ultrasound* 1991;19:215-220
19. Inampudi P, Jacobson JA, Fessell DP, Carlos RC, Patel SV, Delaney-Sathy LO, et al. Soft-tissue lipomas: accuracy of sonography in diagnosis with pathologic correlation. *Radiology* 2004;233:763-767
20. Lee MH, Kim NR, Ryu JA. Cyst-like solid tumors of the musculoskeletal system: an analysis of ultrasound findings. *Skeletal Radiol* 2010;39:981-986
21. Teefey SA, Dahiya N, Middleton WD, Gelberman RH, Boyer MI. Ganglia of the hand and wrist: a sonographic analysis. *AJR*

Am J Roentgenol 2008;191:716-720
22. Feldman MK, Katyal S, Blackwood MS. US artifacts. *Radiographics* 2009;29:1179-1189
23. Huang CC, Ko SF, Huang HY, Ng SH, Lee TY, Lee YW, et al. Epidermal cysts in the superficial soft tissue: sonographic features with an emphasis on the pseudotestis pattern. *J Ultrasound Med* 2011;30:11-17
24. Mendelson EB, Böhm-Vélez M, Berg WA, Whitman GJ, Feldman MI, Madjar H, et al. *ACR BI-RADS ultrasound*. In: D'Orsi CJ, Sickles EA, Mendelson EB, Morris EA, eds. *ACR BI-RADS atlas, breast imaging reporting and data system*, 5th ed. Reston, VA: American College of Radiology, 2013:1-173
25. Chau CL, Griffith JF. Musculoskeletal infections: ultrasound appearances. *Clin Radiol* 2005;60:149-159
26. Chang CD, Wu JS. Imaging of musculoskeletal soft tissue infection. *Semin Roentgenol* 2017;52:55-62
27. Turecki MB, Taljanovic MS, Stubbs AY, Graham AR, Holden DA, Hunter TB, et al. Imaging of musculoskeletal soft tissue infections. *Skeletal Radiol* 2010;39:957-971
28. Chandrasekaran V, Parkash S, Raghuveer CV. Epidermal cysts - a clinicopathological and biochemical study. *Postgrad Med J* 1980;56:823-827
29. Fullen DR. *Cysts and sinuses*. In: Busam KJ, Goldblum JR, eds. *Dermatopathology*, 2nd ed. Philadelphia, PA: Saunders, 2016:310-336
30. Altman DG, Royston P. What do we mean by validating a prognostic model? *Stat Med* 2000;19:453-473
31. Steyerberg EW, Bleeker SE, Moll HA, Grobbee DE, Moons KG. Internal and external validation of predictive models: a simulation study of bias and precision in small samples. *J Clin Epidemiol* 2003;56:441-447
32. Yoon JH, Lee HS, Kim EK, Moon HJ, Kwak JY. A nomogram for predicting malignancy in thyroid nodules diagnosed as atypia of undetermined significance/follicular lesions of undetermined significance on fine needle aspiration. *Surgery* 2014;155:1006-1013
33. Bleeker SE, Moll HA, Steyerberg EW, Donders AR, Derksen-Lubsen G, Grobbee DE, et al. External validation is necessary in prediction research: a clinical example. *J Clin Epidemiol* 2003;56:826-832
34. Steyerberg EW, Vickers AJ, Cook NR, Gerds T, Gonen M, Obuchowski N, et al. Assessing the performance of prediction models: a framework for traditional and novel measures. *Epidemiology* 2010;21:128-138
35. Widmann G, Riedl A, Schoepf D, Glodny B, Peer S, Gruber H. State-of-the-art HR-US imaging findings of the most frequent musculoskeletal soft-tissue tumors. *Skeletal Radiol* 2009;38:637-649
36. Elston DM. *Benign tumors and cysts of the epidermis*. In: Elston DM, Ferringer T, Ko CJ, Peckham S, High WA, DiCaudo DJ, eds. *Dermatopathology*, 3rd ed. New York, NY: Elsevier, 2019:36-53
37. Stavros AT. *Sonographic evaluation of breast cysts*. In: Stavros AT, ed. *Breast ultrasound*. Philadelphia, PA: Lippincott Williams & Wilkins, 2004:276-350
38. Giess CS, Raza S, Birdwell RL. Distinguishing breast skin lesions from superficial breast parenchymal lesions: diagnostic criteria, imaging characteristics, and pitfalls. *Radiographics* 2011;31:1959-1972
39. Yuan WH, Hsu HC, Lai YC, Chou YH, Li AF. Differences in sonographic features of ruptured and unruptured epidermal cysts. *J Ultrasound Med* 2012;31:265-272
40. Jin W, Ryu KN, Kim GY, Kim HC, Lee JH, Park JS. Sonographic findings of ruptured epidermal inclusion cysts in superficial soft tissue: emphasis on shapes, pericystic changes, and pericystic vascularity. *J Ultrasound Med* 2008;27:171-176; quiz 177-178

 https://doi.org/10.3348/kjr.2019.0241